

# Stability of Jahn-Teller distortion in $\text{LaMnO}_3$ under pressure: An x-ray absorption study

Aline Y. Ramos\* and Hélio C. N. Tolentino

*Institut Néel, UPR 2940-CNRS, 25 av. des Martyrs, Boîte Postale 166, 38042 Grenoble, France  
and Laboratório Nacional de Luz Síncrotron-LNLS, P.O. Box 6192, 13084-971, Campinas, São Paulo, Brazil*

Narcizo M. Souza-Neto

*Laboratório Nacional de Luz Síncrotron-LNLS, P.O. Box 6192, 13084-971, Campinas, São Paulo, Brazil  
and Departamento de Física dos Materiais e Mecânica, DFMT-IF-USP, São Paulo, SP, Brazil*

Jean-Paul Itié

*Synchrotron SOLEIL, L'Orme des Merisiers, Saint-Aubin, Boîte Postale 48, 91192 Gif-sur-Yvette Cedex, France*

Liliana Morales and Alberto Caneiro

*Centro Atómico Bariloche and Instituto Balseiro, Comisión Nacional de Energía Atómica and Universidad Nacional de Cuyo,  
8400 S.C. de Bariloche, Argentina*

(Received 23 November 2006; revised manuscript received 20 December 2006; published 12 February 2007)

The local environment of manganese atoms in  $\text{LaMnO}_3$  under pressure up to 15.3 GPa has been studied by x-ray absorption spectroscopy. For pressures below 8 GPa, no change is detected within the  $\text{MnO}_6$  octahedra. Above this pressure a continuous reduction of the long Mn-O distance takes place, however, the octahedral distortion persists over the whole pressure range. At 15.3 GPa the average Jahn-Teller splitting of the distances is reduced by about one-third, indicating that a total removal of the local Jahn-Teller distortion would occur only for pressures around 30 GPa, where metallization is reported to take place. A hysteresis in the long distance reduction is observed down to ambient pressure, suggesting the coexistence of  $\text{MnO}_6$  distorted and undistorted units.

DOI: [10.1103/PhysRevB.75.052103](https://doi.org/10.1103/PhysRevB.75.052103)

PACS number(s): 61.50.Ks, 61.10.Ht, 75.47.Lx, 71.30.+h

The physics underlining the remarkable properties of the manganite  $\text{LaMnO}_3$  and its doped alloys is rich and complex. The actual path followed by a given system towards ferromagnetism and/or metallization, through chemical substitution, thermal treatment, or pressure involves modifications of a delicate balance between delocalization and carriers trapping not yet completely understood. In the ground state  $\text{LaMnO}_3$  is an antiferromagnetic semiconductor crystallizing in an orthorhombic variant of the cubic perovskite structure space group  $Pbnm$ . The  $\text{MnO}_6$  octahedra are distorted due to the Jahn-Teller (JT) effect of the  $\text{Mn}^{3+}(t_{2g}^3 e_g^1)$  and the Mn-O distances are split into four short bonds and two long bonds. In the basal  $ab$  plane long and short Mn-O bonds alternate. The apical and basal short bonds have different length, however, this additional distortion is not resolved by local probes such as real space high resolution diffraction and x-ray absorption spectroscopy. The local radial distribution actually seen by these probes corresponds then to the JT splitting, with four oxygens at short distances  $(\text{Mn-O})_s \approx 1.94 \text{ \AA}$  and two oxygens at the long distance  $(\text{Mn-O})_l \approx 2.15 \text{ \AA}$ .  $\text{LaMnO}_3$  undergoes a transition at  $T^* \approx 710\text{--}750 \text{ K}$  from the JT distorted orthorhombic phase O to a high temperature nearly cubic O' phase.<sup>1</sup> The transition is accompanied by abrupt changes in the electrical resistivity and Weiss constant.<sup>2</sup> The cell distortion is nearly removed and the orbital ordering disappears in the O' phase, but the JT distortion of  $\text{MnO}_6$  octahedra persists at the local scale.<sup>3-5</sup> The transition then happens as an order-disorder transition, in agreement with the thermodynamic calculations.<sup>6</sup> More recently Qiu and co-workers<sup>7</sup> reported on neutron powder dif-

fraction measurements showing that the JT distortion of  $\text{MnO}_6$  octahedra is maintained also in the high temperature rhombohedral phase ( $T \geq 1010 \text{ K}$ ) and suggested the presence of ordered clusters with strong antiferrodistorsive coupling.

New insights for the role of the JT distortion can be obtained by the exploration of its pressure dependence. In  $\text{LaMnO}_3$ , the application of an external hydrostatic pressure produces a reduction of the lattice distortions and an enhancement of the carrier mobility.<sup>8,9</sup> The Mn-O-Mn angle—tilt angle among two adjacent octahedra—is reported to decrease monotonically. The short bond distances  $(\text{Mn-O})_s$  are weakly shortened with increasing pressure, the largest effect being a shortening of the long distance  $(\text{Mn-O})_l$ . Besides, resistivity measurements<sup>8</sup> reveal that the system keeps its insulating nature at room temperature up to 32 GPa where it undergoes an insulator-metal transition. From the extrapolation of x-ray diffraction data, it has been inferred that local JT distortion completely vanishes around 18 GPa.<sup>8</sup> However, *ab initio* calculations using soft pseudopotentials recently predicted the conservation of local octahedral distortion well above this value.<sup>10</sup> The authors predict the occurrence of a structural phase transition around 15 GPa leading to a situation with a mixture of polytypes of antiferromagnetic order.<sup>11</sup> Based on mean field theoretical calculations, Yamasaki and co-workers<sup>12</sup> also claimed that pressure-induced metal-to-insulator transition in  $\text{LaMnO}_3$  is not of Mott Hubbard type. They show that, according to calculations combining local density approximations and mean field theories, both on site repulsion and Jahn-Teller distortion are necessary for

LaMnO<sub>3</sub> to be insulating below 32 GPa. The issue of local distortion in LaMnO<sub>3</sub> at high pressure is then not fully addressed.

Although the use of x-ray absorption spectroscopy (XAS) has been conclusive to elucidate many critical points of the local structure of LaMnO<sub>3</sub> and its doped alloys,<sup>13–16</sup> no pressure dependence of the local order has been reported yet by XAS measurements, neither in the XANES (x-ray absorption near edge structure) nor in the EXAFS (extended x-ray absorption fine structure) range. This is principally due to inherent experimental difficulties in the collection of the XAS high pressures data at the manganese *K* edge, arising both from the low transmission of the diamond cells and from the strong additional absorption due to the La *L* edges. These difficulties were partially overcome here by using perforated-diamond cell<sup>17,18</sup> and taking advantage of the high stability of a dispersive XAS setup. This setup is based on a bent crystal monochromator that opens up the energy bandpass necessary for the spectroscopy and focuses it to the sample position. The dispersing bandpass is collected by a linear detector giving rise to a full spectrum at once. There is no moving optical element during experiments and an extremely good accuracy in the energy scale can be achieved.<sup>19</sup> Above 8 GPa the long distance (Mn-O)<sub>l</sub> is continuously reduced, however, an octahedral distortion persists over the whole pressure range. A hysteresis in the long distance reduction is observed down to ambient pressure, suggesting the coexistence of MnO<sub>6</sub> distorted and undistorted units.

The pressure dependent x-ray absorption measurements at the Mn *K* edge were performed at the XAS dispersive beamline<sup>20</sup> of the LNLS (Laboratório Nacional de Luz Síncrotron, Campinas, Brazil). A polycrystalline powder sample of LaMnO<sub>3</sub> was synthesized by the liquid-mix method previously described.<sup>21</sup> The as-made sample was annealed at  $T = 1000$  °C under oxygen partial pressure  $p(\text{O}_2)$  during 24 h and then quenched at liquid nitrogen temperature. The  $T$  and  $p(\text{O}_2)$  values were chosen in order to give an LaMnO<sub>3</sub> oxygen stoichiometric compound, according to high temperature thermodynamic measurements.<sup>22</sup> The lattice parameters obtained from the Rietveld refinement agree with those of literature.<sup>23</sup> A fine grained powder sample was loaded in a 100 μm diameter hole of an iconel gasket mounted on perforated diamond as support to the 500 μm thick diamond anvils.<sup>18</sup> Silicone oil was used as pressure transmissive medium. Quasi-hydrostatic pressures up to 15.3 GPa were applied and controlled using ruby sphere with a precision of about 0.5 GPa. For each pressure, the cell was then realigned at the optical focus—of around 150 μm—and the spectra were collected in the transmission geometry. The beam path was set under vacuum, to reduce air absorption and beam harmonic contamination. To ensure the beam harmonic purity an additional gold coated mirror was added just behind the anvil cell and set to a grazing angle of 8 mrad. The energy resolution was about 1.5 eV, with energy calibration stable within 0.05 eV during the experiments.

The XANES spectra collected at various pressures exhibit slight modifications (Fig. 1), indicating that the local atomic manganese environment is not drastically changed under external hydrostatic pressure. For pressures up to 8 GPa, no change at all is detected within the MnO<sub>6</sub> octahedra. In this

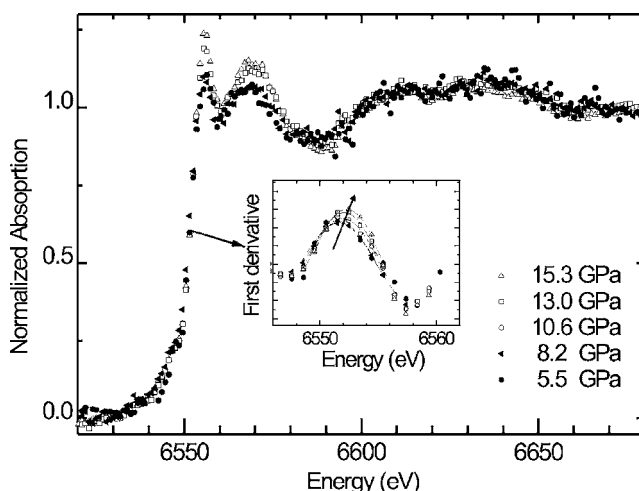


FIG. 1. Mn *K* edge XANES spectra for LaMnO<sub>3</sub> at increasing pressures. Up to 8 GPa, the XANES are unchanged. Above 8 GPa, the structures just beyond the edge (6650–6680 eV) are slightly enhanced, whereas the absorption threshold is continuously shifted towards higher energies. The inset shows the spectra derivatives for a best observation of this last effect.

pressure range a reduction of the cell volume has been observed by x-ray and neutron diffraction measurements.<sup>8,9</sup> A continuous decrease of the Mn-O bond length from ambient pressure to 8 GPa is also reported. Even when sharply contrasted there may not be contradiction between the diffraction and the XAS results. On the one hand XRD provides the static periodicity of the structure averaged over a large spatial domain. On the other hand, as the characteristic time in the photoabsorption process is smaller than that the time corresponding to the thermal motion of the atomic bonds, XAS probes the instantaneous short range structure around the absorbing atoms. The shining example is LaMnO<sub>3</sub> on crossing the Jahn-Teller transition temperature. Diffraction methods show that the three bonds converge into a single bond length on crossing  $T^*$ , whereas XAS gives no change at all in the three bond lengths.<sup>3–5</sup> The dynamic nature of the Jahn-Teller transition has been deduced from the confrontation of both experimental evidences. By analogy with the temperature dependent measurements, we may assume here that when an external pressure above 8 GPa is applied the main effect should be then the rearrangement among the octahedra, with possibly the formation of domains of disordered distortions, while the local instantaneous octahedron keeps almost unchanged. Such rearrangement would result in a reduction of the coherence length of the dynamical spatial fluctuations, and yield, in diffraction measurements, to the derivation of smaller average static values for the Mn-O bonds.

Above 8 GPa, we observe a continuous shift of the absorption threshold towards higher energies (Fig. 1 and inset), along with the enhancement of the structures just above the edge (6650–6680 eV). As the manganese formal valence (Mn<sup>3+</sup>) keeps unchanged with pressure, the edge shift ( $\delta E$ ) expresses here modifications in the repulsive nearest neighbors potential arising from change in Mn-O bonds in the coordination shell.<sup>24</sup> Besides, as shorter bond lengths corre-

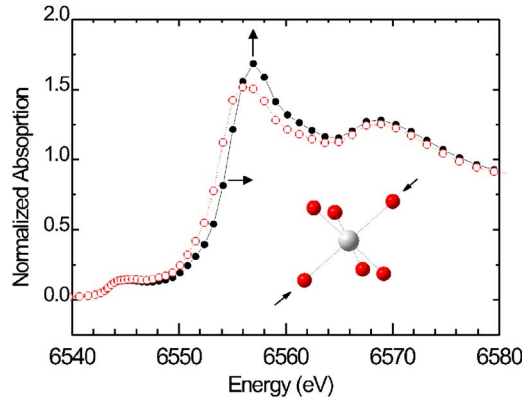


FIG. 2. (Color online) XANES simulations. Open symbols: LaMnO<sub>3</sub> structure. Closed symbols: LaMnO<sub>3</sub> variant where the (Mn-O)<sub>l</sub> bonds are reduced ( $\approx 0.1$  Å). The edge is shifted ( $\approx 0.9$  eV) and the structures above the edge are enhanced.

spond to higher edge energies, the edge position is determined by the long distance (Mn-O)<sub>l</sub>  $\approx 2.15$  Å.  $\delta E$  is then here essentially related to the specific reduction in this bond. At the same time, the structures close to the edge are enhanced. It should be pointed out that, due to the selection rules in x-ray absorption spectroscopy, the *K* edge transition originates from the core *1s* state to the projected *np* (mainly *4p*) unoccupied states. The enhancement in the structures close to the edge accounts for a change in the hybridization concomitant with the increasing overlap of the wave functions when the hydrostatic pressure is applied. This indicates a reduction of the local distortion of the Mn sites, leading to a reduction of the *e<sub>g</sub>* splitting and a partial delocalization of the *e<sub>g</sub>* electrons. Our results then agree with the intuitive idea, also confirmed by the x-ray diffraction measurements,<sup>8,9</sup> that the short bonds (Mn-O)<sub>s</sub> should be less reduced than the long (Mn-O)<sub>l</sub> ones by the application of an external pressure.

*Ab initio* XANES calculations<sup>25</sup> of LaMnO<sub>3</sub>-based structures with progressive reduction of the (Mn-O)<sub>l</sub> bond reproduce well the experimental features (Fig. 2). We should report that in simulations where long and short bonds are reduced in the same proportion, the positive edge shift is correctly reproduced but the structures at the edge are not enhanced. The evolution of the XANES features reflects then a continuous reduction of the average JT distortion from 8 GPa up to 15.3 GPa. The evolution of the edge energy as a function of the applied pressure is given in Fig. 3. For small shifts the relationship between the reduction  $\delta R$  of a bond distance and the associated edge shift  $\delta E$  is almost linear.<sup>24</sup> An experimental calibration obtained for manganite systems<sup>26</sup> gives  $\frac{\delta E}{\delta R} \approx 10$  eV/Å. We also obtain the similar calibration from our XANES simulations ( $\frac{\delta E}{\delta R} \approx 9$  eV/Å, Fig. 2).

The edge shift of 0.6 eV from 8 to 15.3 GPa corresponds then to a reduction in the long bond (Mn-O)<sub>l</sub> by about  $0.06 \pm 0.02$  Å over this range. Even if the short bonds (Mn-O)<sub>s</sub> were not reduced at all under pressure, the total suppression of the JT splitting would result in an energy shift at the edge of the order of 2 eV, which is not observed. Up to

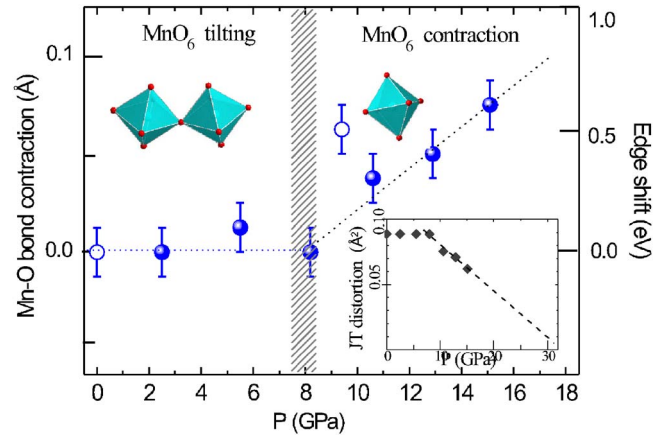


FIG. 3. (Color online) Relative changes in Mn-O distance in the pressure range 0–15.3 GPa. The closed circles are obtained by increasing the pressure and the open circles correspond to the release. The curve in the inset gives an estimation of the JT distortion defined by  $(\sigma_{JT})^2 = (\sqrt{1/6} \sum |R_i - R|)^2$  and predicts a suppression of the distortion above 30 GPa.

15 GPa, the coherent JT distortion parameter  $(\sigma_{JT})^2$ —defined as  $\sigma_{JT} = \sqrt{1/6} \sum |R_i - R|$ —decreases only by one-third (Fig. 3, inset). Local JT distortions are then present, even if the crystallographic structure suggests otherwise. Extrapolation of the data shows that the JT splitting would vanish only around 30 GPa, i.e., for applied pressures where the system is reported to undergo an insulator-metal transition.<sup>8</sup>

When the pressure is released down to ambient, a hysteresis is observed. At 9 GPa all features of the XANES spectrum are similar to those of the spectra at 13 GPa. Such hysteresis suggests the occurrence of a mixture of phases with close compositions and related structures.<sup>27</sup> The hysteresis results in this case from the non-negligible elastic strain energy of coherent or semicoherent interfaces that must be taken into account to describe the total Gibbs energy of the system. As the free motion of each MnO<sub>6</sub> octahedron is limited by the oxygen atoms shared with the adjacent units, electron phonon coupling may involve several coupled Mn atoms.<sup>28</sup> We should remind the reader that XAS informs on the average Mn environment. The present data may then be examined considering that application of the pressure above 8 GPa would induce the progressive formation of MnO<sub>6</sub> undistorted units coupled to distorted ones. The coexistence, at high pressures, of these larger polarons with the small MnO<sub>6</sub> JT distorted octahedra may account for the hysteresis behavior.

In summary, we studied the modifications in the average local distortion around the manganese atoms induced by application of high pressures in the range 0–15.3 GPa, from the modifications of x-ray absorption spectra in the near edge range. The MnO<sub>6</sub> octahedra keep unchanged by application of hydrostatic pressures up to 8 GPa, whereas above this value the long (Mn-O)<sub>l</sub> distance is continuously reduced. The Jahn-Teller bond splitting persists over the whole pressure range. The total quenching of this splitting is expected to take place only at pressures above 30 GPa, indicating that local JT distortion and insulator-to-metal transition should be

closely related. A hysteresis in the XANES features when pressure is released suggests the coexistence of  $\text{MnO}_6$  distorted and undistorted units.

This work was partially supported by a LNLS/ABTLuS/MCT, CNPq, and CNPq-CNRS agreement.

---

\*Electronic address: aline.ramos@grenoble.cnrs.fr

- <sup>1</sup>J. Rodríguez-Carvajal, M. Hennion, F. Moussa, A. H. Moudden, L. Pinsard, and A. Revcolevschi, *Phys. Rev. B* **57**, R3189 (1998).
- <sup>2</sup>J.-S. Zhou and J. B. Goodenough, *Phys. Rev. B* **60**, R15002 (1999).
- <sup>3</sup>E. Araya-Rodríguez, A. Y. Ramos, H. C. N. Tolentino, E. Granada, and S. Oseroff, *J. Magn. Magn. Mater.* **233**, 88 (2001).
- <sup>4</sup>M. C. Sánchez, G. Subías, J. García, and J. Blasco, *Phys. Rev. Lett.* **90**, 045503 (2003).
- <sup>5</sup>R. A. Souza, N. M. Souza-Neto, A. Y. Ramos, H. C. N. Tolentino, and E. Granada, *Phys. Rev. B* **70**, 214426 (2004).
- <sup>6</sup>A. J. Millis, *Phys. Rev. B* **53**, 8434 (1996).
- <sup>7</sup>X. Qiu, T. Proffen, J. F. Mitchell, and S. J. L. Billinge, *Phys. Rev. Lett.* **94**, 177203 (2005).
- <sup>8</sup>I. Loa, P. Adler, A. Grzechnik, K. Syassen, U. Schwarz, M. Hanfland, G. K. Rozenberg, P. Gorodetsky, and M. P. Pasternak, *Phys. Rev. Lett.* **87**, 125501 (2001).
- <sup>9</sup>L. Pinsard-Gaudart, J. Rodríguez-Carvajal, A. Daoud-Aladine, I. Goncharenko, M. Medarde, R. I. Smith, and A. Revcolevschi, *Phys. Rev. B* **64**, 064426 (2001).
- <sup>10</sup>G. Trimarchi and N. Binggeli, *Phys. Rev. B* **71**, 035101 (2005).
- <sup>11</sup>T. Mizokawa, D. I. Khomskii, and G. A. Sawatzky, *Phys. Rev. B* **60**, 7309 (1999).
- <sup>12</sup>A. Yamasaki, M. Feldbacher, Y.-F. Yang, O. K. Andersen, and K. Held, *Phys. Rev. Lett.* **96**, 166401 (2006).
- <sup>13</sup>T. A. Tyson, J. MustredeLeon, S. D. Conradson, A. R. Bishop, J. J. Neumeier, H. Röder, and J. Zang, *Phys. Rev. B* **53**, 13985 (1996).
- <sup>14</sup>G. Subías, J. García, M. G. Proietti, and J. Blasco, *Phys. Rev. B* **56**, 8183 (1997).
- <sup>15</sup>C. H. Booth, F. Bridges, G. H. Kwei, J. M. Lawrence, A. L. Cornelius, and J. J. Neumeier, *Phys. Rev. B* **57**, 10440 (1998).
- <sup>16</sup>T. Shibata, B. A. Bunker, and J. F. Mitchell, *Phys. Rev. B* **68**, 024103 (2003).
- <sup>17</sup>A. Dadashev, M. P. Pasternak, G. K. Rozenberg, and R. Taylor, *Rev. Sci. Instrum.* **72**, 2633 (2001).
- <sup>18</sup>J. P. Itié, F. Baudalet, A. Congeduti, B. Couzinet, F. Farges, and A. Polian, *J. Phys.: Condens. Matter* **17**, S883 (2005).
- <sup>19</sup>H. Tolentino, E. Dartyge, A. Fontaine, and G. Tourillon, *J. Appl. Crystallogr.* **21**, 15 (1988).
- <sup>20</sup>H. C. N. Tolentino, J. C. Cezar, N. Watanabe, C. Piamonteze, N. M. Souza-Neto, E. Tamura, A. Y. Ramos, and R. Neueschwander, *Phys. Scr.* **115**, 977 (2005).
- <sup>21</sup>F. Prado, R. D. Sanchez, A. Caneiro, M. T. Causa, and M. Tovar, *J. Solid State Chem.* **146**, 418 (1999).
- <sup>22</sup>L. Morales and A. Caneiro, *J. Solid State Chem.* **170**, 404 (2003).
- <sup>23</sup>F. Prado, R. Zysler, L. Morales, A. Caneiro, M. Tovar, and M. T. Causa, *J. Magn. Magn. Mater.* **196**, 481 (1999).
- <sup>24</sup>C. Natoli, in *EXAFS and Near Edge Structure III*, edited by B. H. K. O. Hodgson and J. Penner-Hahn, Springer Proceedings in Physics Vol. 2 (Springer-Verlag, Berlin, 1984), pp. 38–42.
- <sup>25</sup>A. L. Ankudinov, B. Ravel, J. J. Rehr, and S. D. Conradson, *Phys. Rev. B* **58**, 7565 (1998).
- <sup>26</sup>N. M. Souza-Neto, A. Y. Ramos, H. C. N. Tolentino, E. Favre-Nicolin, and L. Ranno, *Phys. Rev. B* **70**, 174451 (2004).
- <sup>27</sup>N. Grunbaum, L. Moggi, F. Prado, and A. Caneiro, *J. Solid State Chem.* **177**, 2350 (2004).
- <sup>28</sup>M. C. Sánchez, J. García, G. Subías, and J. Blasco, *Phys. Rev. B* **73**, 094416 (2006).